CHARACTERIZING GLOBAL INTER-ANNUAL DUST REMOVAL AND DEPOSITION USING THERMAL EMISSION IMAGING SYSTEM (THEMIS) INFRARED DATA C. A. Wolfe[1], C. S. Edwards[1], S. Piqueux[2], [1]Northern Arizona University, Flagstaff, AZ 86011, [2]Jet Propulsion Laboratory, California Institute of Technology, Pasadena, CA 91109, cw997@nau.edu

Introduction: Dust is ubiquitous on Mars and is constantly altering the appearance of both the atmosphere and surface. Aside from modifying the overall look of the planet, dust plays a key role in a variety of atmospheric and surface processes. While the atmosphere of Mars typically contains dust throughout the year, atmospheric dust load varies considerably from season to season. The amount of dust in the atmosphere influences the degree to which solar and infrared radiation are absorbed and scattered, controlling the atmospheric temperature of Mars and thus global circulation patterns [1]. Globally, it is estimated that 2.9×10^{12} kg/yr of dust is exchanged between the surface and atmosphere of Mars [2], making dust transport one of the most dynamic and prevalent geological processes occurring on present-day Mars.

The observed Martian dust cycle depends heavily on the availability of mobile dust particles at the surface [3]. Dust is currently deposited uniformly throughout the equatorial region at a rate of $\sim$ 40 μm/global storm, but over geologic timescales, the rate of accumulation may vary from 0 to 250 μm/yr due to changes in atmospheric conditions produced by orbital variations [4]. Dust deposited during global dust storms is generally observed to be removed from only dark, high thermal inertia regions, thus resulting in a net accumulation of dust in bright, low thermal inertia regions. Surface dust deposits are known to exist on Mars in at least the three low thermal inertia regions of Arabia, Tharsis, and Elysium [4]. Observational estimates of deposition rates in these regions range from a few to almost 50 μm/yr [5], assuming the dust was deposited uniformly.

Context: While variations of the surface albedo and spectral properties linked to dust deposition, transport, and removal are well documented [5] [6] [7] [8], a global scale quantification of surface dust fluxes between dust sources and sinks before, during, and after dust storms has not been carried out to date. Poor constraints on surface dust fluxes not only prevent Global Circulation Model (GCM) simulations from providing accurate results, but impedes any improvement of dust storm prediction and forecasting. This knowledge gap will be addressed by characterizing the fine-scale ($\sim$100 m) context for dust migration using THEMIS IR data. More specifically, we will quantify an upper limit on the amount of inter-annual dust (in μm) that was either deposited or removed from a specific region during a particular season and time of day, allowing tighter constraints to be placed on the activity of dust sources and sinks.

Methodology: The inter-seasonal/annual depletion and replenishment of surface dust reservoirs available for dust storm onset and growth leaves a measurable thermophysical signature (i.e. thermal inertia, albedo) that we will quantify and map to constrain the availability of surface dust through time. Image pairs are obtained by querying a variety of acquisition- and observational-based parameters stored in a database containing the entire global THEMIS IR dataset. This query returns a list of both daytime and nighttime data product IDs for images acquired at roughly the same season ($\leq$ 20° L_S) and same local time ($\leq$ 1 hour), but different Mars years. Only image pairs that are well-calibrated and have a regional area overlap greater than 100 km^2 are considered.

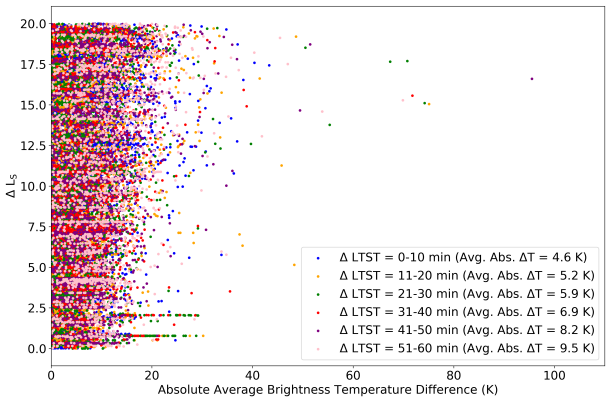

Figure 1: Daytime average brightness temperature difference as a function of L_S difference with colors indicating local time difference (in min.) between images.

After performing the query outlined above, images and relevant metadata are downloaded using Bayleef, a Python library for interfacing with the US Geologic Survey's (USGS) Inventory Service. Images are then processed to correct for instrument noise and other artifacts using the DaVinci software package, following well-established procedures outlined in [9]. After images have been processed, each unprojected image is cropped based on its latitude, returning a geometrically projected image that only spans the overlapping region, thus minimizing the amount of storage space needed and computational time required by ensuing steps.

Once images have been processed and cropped, they are registered to within 0.5 pixels ($\sim$50 m) using a tie-point and bundle adjustment method developed by the

Integrated Software for Imaging Spectrometers (ISIS) [10]. In this step, a control network produces ties (control points) from one image to another (control measures) through a sub-pixel registration algorithm to identify common ground points across each image within a pair. After valid control measures are established, a bundle adjustment routine generates new camera and spacecraft pointing information. This updated pointing information is then used to project the image pairs to their relevant locations on Mars, requiring no further adjustment or warping after the initial projection [9].

After the successful registration and projection of each image, image post-processing and brightness temperature conversion is performed using DaVinci. Only the Band 9 (centered at 12.57 μm) brightness temperature values are used for this investigation. At this wavelength surface emissivity is high ($\sim$ 0.99), atmospheric opacity is low, and the surface-atmosphere temperature contrast is high [9], resulting in a high signal-to-noise ratio for both daytime and nighttime data, and thus accurate surface brightness temperature values.

To properly identify the inter-annual/seasonal variability present within the image pairs generated, a systematic method to reliably assess image-image variability was performed. After converting each pixel's spectral radiance to a brightness temperature, a variety of useful statistics are collected, including the minimum, maximum, average, and standard deviation brightness temperature differences, as well as the number of pixels over specific thresholds. To further help identify and characterize changes in brightness temperature that may be the result of either large- or small-scale thermophysical differences, the average normalized brightness temperature difference is computed for each image pair.

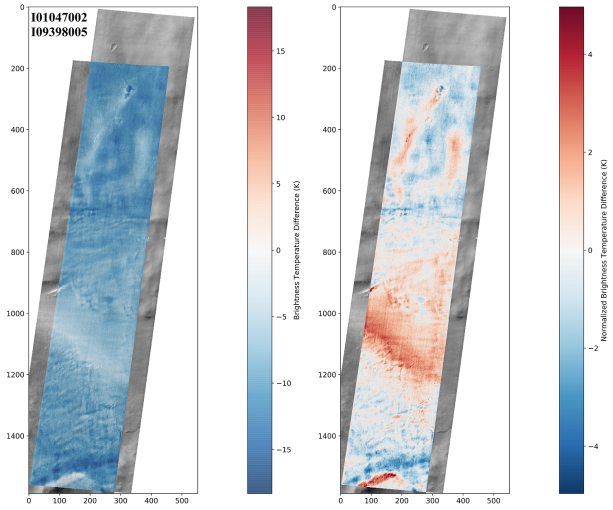

Figure 2: Unnormalized vs. normalized brightness temperature difference for daytime THEMIS image pair.

The KRC thermal model [11] will be employed to simulate a variety of layered surface and subsurface conditions to produce a multidimensional lookup table. Specifically, we are interested in modeling the deposition/removal of a thin layer of fine-grained, low thermal inertia, high albedo dust particles on top a substrate with a higher bulk thermal inertia and lower albedo [12]. Using a host of input parameters, including L_S, latitude, local time, surface albedo, elevation, and dust opacity, surface temperature will be derived for a variety of thermal inertia values, allowing different dust layer thicknesses to be modeled. By comparing modeled surface temperatures with observed values, an upper limit on the amount of dust deposited or removed from the overlapping region can be assigned to each image pair.

Preliminary Results: Of the 114,197 daytime images returned by the database query, 57,098 were successfully co-registered and bundle adjusted. The majority of these image pairs exhibit an average absolute brightness temperature difference of less than 20 K. As illustrated by Figure 1, a significant correlation does not appear to exist between average brightness temperature difference and season/local time difference. This is expected as keeping seasonal and local time differences between images small reduces the impact surface and sub-surface heterogeneities may have on surface thermal inertia, and thus brightness temperature. Deviations from a climatologically average Mars year will thus yield significant brightness temperature differences between images.

We have successfully demonstrated that smaller, more localized features are capable of being captured from bulk temperature differences by normalizing an image pair, with Figure 2 providing an example. While the unnormalized pair on the left exhibits a relatively homogeneous surface temperature decrease of $\sim$ 9 K, the normalized version reveals small-scale fluctuations, which may provide clues on how much dust was deposited or removed from the overlapping region. One likely scenario is that dust was deposited unevenly across the region, leading to an increase in surface albedo, and thus a decrease in brightness temperature. Constraining dust fluxes at such a high spatial resolution will allow sources and sinks to be constrained with much greater accuracy.

References: [**1**] Ryan J.A. and Henry R.M, *JGR: Solid Earth*, 1979, [**2**] Pollack J.B. et al., *JGR*, 1977, [**3**] Kahre M.A. et al., *JGR: Planets*, 2006, [**4**] Christensen P.R., *JGR: Solid Earth*, 1986, [**5**] Christensen P.R., *JGR: Solid Earth*, 1988, [**6**] Vincendon M. et al. *Icarus*, 2015, [**7**] Wells E.N. et al., *Icarus*, 1984, [**8**] Szwast M.A. et al., *JGR: Planets*, 2006, [**9**] Edwards C.S. et al., *JGR: Planets*, 2011, [**10**] Gaddis L. et al., *LPSC*, 1997, [**11**] Kieffer H.H., *JGR: Planets*, 2013, [**12**] Edwards C.S. et al., *JGR: Planets*, 2011.